Available online at www.sciencedirect.com
ScienceDirect
Journal of the Mechanics and Physics of Solids 56 (2008) 1018–1042
JOURNAL OF THE MECHANICS AND PHYSICS OF SOLIDS
www.elsevier.com/locate/jmps

# Reversible magneto-elastic behavior: A multiscale approach

Laurent Daniel[a,*], Olivier Hubert[b], Nicolas Buiron[c], René Billardon[b]

[a]LGEP - CNRS (UMR 8507), Supélec, Univ Paris-Sud, UPMC-Paris6 Plateau du Moulon, 91192 Gif sur Yvette Cedex, France
[b]LMT-Cachan, ENS Cachan, CNRS (UMR 8535), UPMC-Paris6 61 avenue du Président Wilson, 94235 CACHAN Cedex, France
[c]Laboratoire Roberval, Université de Technologie de Compiègne BP 20529, 60205 COMPIEGNE Cedex, France

Received 5 February 2007; received in revised form 7 June 2007; accepted 11 June 2007

**Abstract**

Magnetic and mechanical behaviors are strongly coupled. But few models are able to describe magneto-mechanical coupling effects. We propose a multiscale approach for the modeling of the reversible magneto-elastic behavior of ferromagnetic materials. This approach stands between macroscopic phenomenological modeling and micromagnetic simulations. We detail first the definition of the magneto-elastic behavior of a single crystal, deduced from energetic considerations made at the scale of magnetic domains and hypotheses concerning the domains microstructure. This model is then applied to the description of the behavior of polycrystalline media, through a multiscale approach. The heterogeneity of stress and magnetic field is taken into account through a self-consistent localization–homogenization scheme, including crystallographic texture data. Results are discussed and compared to experimental data from the literature.


*Keywords:* Magneto-elastic couplings; Magnetostriction; Multiscale modeling; Single crystal; Polycrystal

## 1. Introduction

Ferro- and ferrimagnetic materials are used to produce and to transform energy or build actuators. The search for higher performance and lighter electrotechnical devices leads to a deeper need of predictive dimensioning tools, concerning optimization of materials, structures and forming processes. Consequently, advanced models are needed to describe the magnetic behavior. Especially, the accuracy of modeling has to be improved to account for coupled magneto-mechanical phenomena. This coupling is characterized by the influence of stress state on the magnetic susceptibility and by the magnetostriction[1] (i.e. the spontaneous deformation due to magnetization, Joule, 1847; Bozorth, 1951; Du Trémolet de Lacheisserie, 1993). These phenomena are linked to the existence of a magnetic domains microstructure (Hubert and Schäfer, 1998). Each magnetic domain is associated to a given saturation magnetization and magnetostriction strain. Macroscopic magnetization process and magnetostriction are explained by a variation in volume of domains

*Corresponding author. Tel.: +33 1 69 85 16 39; fax: +33 1 69 41 83 18.
*E-mail address:* laurent.daniel@lgep.supelec.fr (L. Daniel).

[1]The form effect will not be addressed in that paper. This elastic deformation—superimposed to the magnetostriction strain—results from the existence of magnetic forces, and is linked to boundary conditions and to the geometry of the considered specimen. Thus, it cannot be introduced into a magneto-elastic constitutive law.

0022-5096/$ - see front matter © 2007 Elsevier Ltd. All rights reserved.
doi:10.1016/j.jmps.2007.06.003

submitted to a magnetic field or stress. A concomitant magnetization process consists in a rotation of magnetization direction of the magnetic domains. A stress modifies the energetic equilibrium of domains structure as well, bringing a change of their volume, and as a consequence a change of susceptibility. At the macroscopic scale, the magnetostriction partly explains the noise emitted by electrical devices, and particularly transformers. The effect of stress on the magnetic behavior is responsible for the decrease of rates in electrical devices submitted to stress. The magnetic behavior cannot, therefore, be accurately determined unless the mechanical fields are taken into account. The difficulty of such a determination is increased by the multiaxiality of magnetic and mechanical loadings.

Up to now, two main approaches have been proposed to describe such coupling effects. On the one hand, several phenomenological macroscopic models (introducing the stress as a parameter in classical macroscopic models) have been proposed, extended from the Jiles–Atherton model (see for instance Sablik and Jiles, 1993), from the Preisach model (for instance Appino et al., 1999 or Bernard and Ossart, 2004) or based on thermodynamic arguments (for instance Hirsinger et al., 2000 or Azoum et al., 2004). The applicability of such approaches is often limited to a short range of loadings, to isotropic materials, and the multiaxiality of stress state is rarely accounted for. Moreover, these approaches do not allow the investigation of materials properties optimization, since the effect of a change in composition or crystallographic texture cannot be predicted. On the other hand, micromagnetic simulations allow the simulation of complex domain structures (DeSimone et al., 2000). They are based on the minimization of the potential energy of the single crystal modeled by a set of interacting magnetic moments, each of them representing a set of atoms. The number of degrees of freedom and interactions is growing very quickly with the number of magnetic moments, so that these simulations are always made for small size systems. Several authors have developed some magneto-elastic simulations that take into account uniaxial or cubic crystalline symmetries (for example He, 1999; DeSimone and James, 2002). This kind of strategy usually concerns 2D patterns and often leads to prohibitive calculation times, still not reasonable today concerning polycrystalline media.

Micro–macro approaches have been successfully developed in many fields of physics during the past years to deduce the overall behavior of heterogeneous materials from the behavior of their constituents. Concerning non-linear behaviors, these approaches have been developed first in the framework of polycrystals plasticity (Hill, 1965; Berveiller and Zaoui, 1978). Applications to coupled phenomena have been proposed for shape memory or ferroelectric polycrystals (see for instance Patoor et al., 2006; Lagoudas et al., 2006; Huber et al., 1999; Haug et al., 2007). But few models have been addressed in the framework of magneto-elasticity. The development of such approaches relies on two key points. The first one is the definition of transition scale rules, depending on the microstructure of the studied material, and allowing to estimate the fluctuation of the local fields for a given macroscopic loading. The second one is an appropriate description of the behavior of the constituents.

Our proposition is to use simplifying hypotheses allowing a fast estimation for the magneto-elastic behavior. Several scales can be chosen to define this behavior, leading to a multiscale calculation strategy, remaining in the framework of continuum mechanics. The first scale for which homogeneous magnetic and mechanical state can be considered is the magnetic domains scale. The next scale is the grain scale for which the elastic properties are homogeneous. We then define the polycrystalline representative volume element (RVE) scale. The studied zone is then large enough to consider that the RVE behavior defines the average material behavior and/or properties. It is not possible to define precisely this scale as its dimensions depend on the studied material and/or on the studied properties.

The polycrystal is seen as a single crystals aggregate, with respect to a given orientation distribution function (ODF), representative of the polycrystal texture. The proposed modeling considers homogeneous magnetic field and strain state within the single crystal. These hypotheses are maintained in each grain of a polycrystal. The fluctuations of magnetic field and stress within the polycrystal is not neglected since they significantly affect the predicted value for the magnetostriction strain. The self-consistent approach (Bruggeman, 1935; Hill, 1965), known to be suitable to polycrystals behavior (Bornert et al., 2007), will be used. Hypotheses of homogeneity of stress and magnetic field will be nevertheless used in order to obtain faster results in the framework of simplified approaches.

Hysteretic phenomena are not considered in this first approach. The proposed modeling is only relevant for reversible magneto-elastic behavior, associated to anhysteretic magnetic field strengthening. Assumptions hereafter have been developed for ferro- or ferrimagnetic materials with a cubic crystallographic symmetry.

The paper is divided into three parts. The first one presents the single crystal constitutive law. The second part is dedicated to the definition of polycrystalline media behavior, with the definition of scale transition rules. In the last part, modeling results are compared to experimental data.

## 2. Single crystals

### 2.1. Energetic equilibrium

At the scale of a group of atoms, the magnetic equilibrium state is the result of the competition between several energetic terms. The potential energy of a group of atoms can be written (Hubert and Schäfer, 1998)

$$W = W_{\mathrm{ex}} + W_{\mathrm{an}} + W_{\mathrm{mag}} + W_{\sigma}, \tag{1}$$

where $W_{\mathrm{ex}}$ denotes the exchange energy; $W_{\mathrm{an}}$ denotes the magneto-crystalline energy; $W_{\mathrm{mag}}$ denotes the magneto-static energy; $W_{\sigma}$ denotes the elastic energy.

#### 2.1.1. Exchange energy

The exchange energy is related to the ferromagnetic coupling effect between neighboring atoms, tending to uniformize the magnetization in a volume element. It can be written

$$W_{\mathrm{ex}} = A(\mathrm{grad}\,\vec{\gamma})^2, \tag{2}$$

$A$ is the exchange constant of the material, and $\vec{\gamma}$ denotes the magnetization direction

$$\vec{M} = M_{\mathrm{s}}\vec{\gamma} \tag{3}$$

$M_{\mathrm{s}}$ is the magnetization saturation value of the material.

Exchange energy is minimum when the spatial variations of the magnetization direction are minimum.

#### 2.1.2. Magneto-crystalline energy

The magneto-crystalline energy tends to force the magnetization to be aligned along particular directions, called easy axes. These directions are mostly connected to crystallographic structure. In the case of cubic crystallographic symmetry, the magneto-crystalline energy can be written

$$W_{\mathrm{an}} = K_0 + K_1(\gamma_1^2\gamma_2^2 + \gamma_2^2\gamma_3^2 + \gamma_3^2\gamma_1^2) + K_2(\gamma_1^2\gamma_2^2\gamma_3^2) \tag{4}$$

$[\gamma_1, \gamma_2, \gamma_3]$ are the direction cosines of $\vec{\gamma}$. $K_0$ is an arbitrary constant, $K_1$ and $K_2$ denote the magneto-crystalline anisotropy constants of the material. Magneto-crystalline energy is minimum when $\vec{\gamma}$ is an easy axis.

#### 2.1.3. Magneto-static energy

The magneto-static energy can be written

$$W_{\mathrm{mag}} = -\mu_0\vec{H}.\vec{M}, \tag{5}$$

$\vec{H}$ and $\vec{M}$ are, respectively, the local magnetic field and magnetization. This term tends to align the magnetization with the magnetic field. It is minimum when $\vec{H} = \|\vec{H}\|\vec{\gamma}$.

#### 2.1.4. Elastic energy

In the case of a linear elastic behavior, Hooke's law defines a proportional relation between elastic strain ($\boldsymbol{\varepsilon}_{\mathrm{e}}$) and stress ($\boldsymbol{\sigma}$). The elastic energy is then defined as

$$W_{\sigma} = \tfrac{1}{2}\boldsymbol{\varepsilon}_{\mathrm{e}} : \mathbb{C}^I : \boldsymbol{\varepsilon}_{\mathrm{e}} = \tfrac{1}{2}\boldsymbol{\sigma} : \mathbb{C}^{-1} : \boldsymbol{\sigma} \tag{6}$$

$\mathbb{C}^I$ is the material stiffness tensor, uniform within a single crystal.

In magnetic materials, the magnetostriction strain[2] $\boldsymbol{\varepsilon}_\mu$ is a source of incompatibility, involved in the definition of $\boldsymbol{\sigma}$ and thus in the definition of $W_\sigma$.

In the case of cubic crystallographic symmetry, the magnetostriction strain $\boldsymbol{\varepsilon}_\mu$ can be described with three parameters. Assuming that this strain is isochore (Du Trémolet de Lacheisserie, 1993), the number of parameters is reduced to two. In the crystallographic frame (CF), the magnetostriction strain tensor can be written

$$\boldsymbol{\varepsilon}_\mu = \frac{3}{2}\begin{pmatrix} \lambda_{100}(\gamma_1^2-\frac{1}{3}) & \lambda_{111}\gamma_1\gamma_2 & \lambda_{111}\gamma_1\gamma_3 \\ \lambda_{111}\gamma_1\gamma_2 & \lambda_{100}(\gamma_2^2-\frac{1}{3}) & \lambda_{111}\gamma_2\gamma_3 \\ \lambda_{111}\gamma_1\gamma_3 & \lambda_{111}\gamma_2\gamma_3 & \lambda_{100}(\gamma_3^2-\frac{1}{3}) \end{pmatrix}_{\mathrm{CF}} \tag{7}$$

where $\lambda_{100}$ and $\lambda_{111}$ denote the magnetostrictive constants. $\lambda_{100}$ (resp. $\lambda_{111}$) is the magnetostriction strain along the direction $\langle 1\,0\,0\rangle$ (resp. $\langle 1\,1\,1\rangle$) of a single crystal when it is magnetized at saturation along this direction.

### 2.2. Definition of the magneto-elastic behavior

If we consider a volume element $V$, the total potential energy becomes

$$W = \frac{1}{V}\int_V (W_{\mathrm{ex}} + W_{\mathrm{an}} + W_{\mathrm{mag}} + W_\sigma)\,\mathrm{d}V. \tag{8}$$

The resolution of a problem of magneto-elasticity involves the minimization of this potential energy for the volume element. This point is the base of the so-called micro-magnetic approaches. The macroscopic quantities ($\boldsymbol{\Sigma}$, $\boldsymbol{E}$, $\vec{M}^{\mathbf{m}}$, $\vec{H}_{\mathbf{ext}}$) are defined by an averaging operation of the local quantities ($\boldsymbol{\sigma}, \boldsymbol{\varepsilon}, \vec{M}, \vec{H}$) over the volume. Such an approach, involving a large number of degrees of freedom, appears to be difficult to implement, particularly if the heterogeneity scale is much smaller than the volume of interest.

In the present case, the volume of interest is the single crystal. If a single crystal is seen as a domains aggregate, the potential energy of a single crystal can be defined as the sum of its domains potential energies and of a wall energy, related to the transition zone between magnetic domains

$$W^{\mathbf{sc}} = \frac{1}{V}\left(\int_{V_{\mathrm{d}}} W^\alpha\,\mathrm{d}V + \int_{V_{\mathrm{w}}} W^{\mathrm{w}}\,\mathrm{d}V\right) \tag{9}$$

$V_{\mathrm{d}}$ being the domains volume and $V_{\mathrm{w}}$ the magnetic walls volume ($V_{\mathrm{d}} + V_{\mathrm{w}} = V$). However, the definition of $W^{\mathrm{w}}$, of the wall volume $V_{\mathrm{w}}$, and of the boundary between domains and walls are quite difficult. Actually, the formulation (9), although seducing, is practically very difficult to use, unless one gets back to a micromagnetic formulation.

We propose a model that uses the uniformity of magnetization and stress in magnetic domains and neglects the fast variations of exchange and magneto-crystalline energies in the domain walls, joining on that point the "no-exchange" formulation (James and Kinderlehrer, 1990; DeSimone, 1993). This model is simple enough to be implemented in a polycrystalline modeling.

### 2.3. Energetic equilibrium of a magnetic domain α and related hypotheses

In a magnetic domain α, with magnetization direction $\vec{\gamma}^\alpha = [\gamma_1, \gamma_2, \gamma_3]$, spatial variations of magnetization are inexistent, the exchange energy is consequently zero.

The magnetization being uniform in a domain, the magneto-crystalline energy is also uniform, and the integration over the volume becomes easy. Eq. (4) remains unchanged

$$W_{\mathrm{an}}^\alpha = K_0 + K_1(\gamma_1^2\gamma_2^2 + \gamma_2^2\gamma_3^2 + \gamma_3^2\gamma_1^2) + K_2(\gamma_1^2\gamma_2^2\gamma_3^2). \tag{10}$$

[2] $\varepsilon_\mu$ denotes the free magnetostriction strain, meaning the magnetostriction strain that would appear if the material was able to deform without any incompatibility.

The magnetic field being supposed uniform in a domain, the magneto-static energy is uniform too, and can be written

$$W^{\alpha}_{\text{mag}} = -\mu_0 \vec{M}^{\alpha}.\vec{H}^{\alpha}, \tag{11}$$

$\vec{H}^{\alpha}$ is the magnetic field at the domain scale. $\vec{M}^{\alpha}$ is the magnetization in the domain, defined by Eq. (12)

$$\vec{M}^{\alpha} = M_s \vec{\gamma}^{\alpha}. \tag{12}$$

A first simplification is related to the definition of the local magnetic field $\vec{H}$. The magneto-static energy is defined assuming that $\vec{H}$ is uniform within a single crystal (or grain) and noted $\vec{H}^{\mathbf{I}}$ ($\vec{H}^{\alpha} = \vec{H}^{\mathbf{I}}$).

A domain is supposed to be a substructure of a zone for which elastic properties are uniform. Magnetostriction strain is also uniform in the domain. We assume that the stress is uniform in a magnetic domain. The elastic energy can then be written

$$W^{\alpha}_{\sigma} = \tfrac{1}{2}\boldsymbol{\sigma}^{\alpha} : \mathbb{C}^{I^{-1}} : \boldsymbol{\sigma}^{\alpha}. \tag{13}$$

A second assumption is related to the expression of the elastic energy. We choose an uniform strain hypothesis within a single crystal, so that the elastic energy expression is simplified (see Appendix A), and can be written

$$W^{\alpha}_{\sigma} = W^{\text{o}}_{\sigma} - \boldsymbol{\sigma}^{I} : \boldsymbol{\varepsilon}^{\alpha}_{\mu}, \tag{14}$$

$\boldsymbol{\sigma}^{I}$ being the mean stress within the single crystal (i.e. the applied stress at the grain scale) and $W^{\text{o}}_{\sigma}$ a constant over the single crystal. The expression obtained by neglecting the constant term is usually called the magneto-elastic energy (Bozorth, 1951; Hubert and Schäfer, 1998)

$$W^{\alpha}_{\sigma\mu} = -\boldsymbol{\sigma}^{I} : \boldsymbol{\varepsilon}^{\alpha}_{\mu}. \tag{15}$$

The potential energy of each domain is then written, except for a constant

$$W^{\alpha} = -\mu_0 \vec{M}^{\alpha}.\vec{H}^{\mathbf{I}} - \boldsymbol{\sigma}^{I} : \boldsymbol{\varepsilon}^{\alpha}_{\mu} + K_1(\gamma_1^2\gamma_2^2 + \gamma_2^2\gamma_3^2 + \gamma_3^2\gamma_1^2) + K_2(\gamma_1^2\gamma_2^2\gamma_3^2). \tag{16}$$

### 2.4. A semi-phenomenological modeling for single crystals

#### 2.4.1. State variables

We consider a single crystal. We define domain families ($\alpha$), each of them being associated to a particular—initial—easy axis ($\vec{\gamma}^{\alpha}_0$).

The chosen state variables are defined for each family and can be divided into two sets:

- The orientation of the magnetization in each domain family, defined by two usual spherical angles $\theta^{\alpha}$ and $\delta^{\alpha}$.
- The volumetric fraction $f^{\alpha}$ of the $\alpha$ domain family in the single crystal.

#### 2.4.2. State variables calculation

Magnetic field and stress tensor being known, the variables $\theta^{\alpha}$ and $\delta^{\alpha}$ are calculated by minimization of the domain potential energy $W^{\alpha}$

$$W^{\alpha}(\theta^{\alpha}, \delta^{\alpha}) = \min(W^{\alpha}). \tag{17}$$

Variables $f^{\alpha}$ cannot be estimated by such a minimization because of the mean magnetic field approach. $f^{\alpha}$ is then obtained using a Boltzmann function,[3] proposed by Buiron et al. (1999) following Chikazumi (1997)

$$f^{\alpha} = \frac{\exp(-A_s.W^{\alpha})}{\sum_{\alpha}\exp(-A_s.W^{\alpha})}, \tag{18}$$

[3]Statistical approach for the determination of a specific state depending on its energy compared to the energy of the other states.

$A_s$ is a parameter that introduces the "inertial" effects ignored by the modeling.[4] Its value can be analytically calculated (see paragraph 2.4.4 and Appendix B). $f^\alpha$ satisfies

$$\sum_\alpha f^\alpha = 1. \tag{19}$$

*2.4.3. Single crystal behavior*

The mean magnetization over the single crystal is defined by

$$\vec{M}^{\mathbf{I}} = \langle \vec{M}^\alpha \rangle = \sum_\alpha f^\alpha \vec{M}^\alpha. \tag{20}$$

Assuming homogeneous elastic properties for the single crystal, the magnetostriction strain can be defined the same way

$$\boldsymbol{\varepsilon}^I_\mu = \langle \boldsymbol{\varepsilon}^\alpha_\mu \rangle = \sum_\alpha f^\alpha \boldsymbol{\varepsilon}^\alpha_\mu. \tag{21}$$

*2.4.4. Identification of $A_s$ parameter*

If the magnetization rotation mechanism is ignored, a simplified modeling can be derived (see Appendix B). This modeling, applicable only for low applied magnetic fields allows to link the parameter $A_s$ to the initial slope of the anhysteretic magnetization curve $\chi^0$. We find

$$A_s = \frac{3\chi^0}{\mu_0 M_s^2}. \tag{22}$$

This parameter is found to be independent of the magnetic field direction. Under this assumption, the only adjustable parameter of the modeling is directly obtained from a single anhysteretic magnetization curve (without mechanical loading).

## 3. Polycrystals

Let us consider a RVE of a polycrystalline material. Grains orientation in the polycrystal is given[5] and the whole properties of the single crystal are known. Depending on these properties and on some hypotheses concerning the microstructure, we want to link the macroscopic response (mean magnetization $\vec{M}^{\mathbf{m}}$ and macroscopic strain $\boldsymbol{E}$) of this RVE to the macroscopic loading (the applied magnetic field $\vec{H}_{\mathbf{ext}}$ and macroscopic stress $\boldsymbol{\Sigma}$). The determination of this constitutive law is based on a localization-homogenization strategy. The generic principle of such a multiscale approach is illustrated on Fig. 1.

### *3.1. Localization scheme*

*3.1.1. Definition of the local stress*

The aim of this step is to derive the local stress $\boldsymbol{\sigma}^I$ from the external loading, postulating a particular form for the function $g$ in relation (23)

$$\boldsymbol{\sigma}^I = g(\boldsymbol{\Sigma}, \vec{H}_{\mathbf{ext}}). \tag{23}$$

The function $g$ is deduced from a self-consistent approach. Each grain is considered as an inclusion in the homogeneous medium equivalent to the polycrystal, so that the problem can be linked to the solution of the Eshelby inclusion problem (Eshelby, 1957).

The magnetostriction strain $\boldsymbol{\varepsilon}^I_\mu$ is considered as a free strain. The Eshelby tensor $\mathbb{S}^E$ is calculated[6] following Mura (1982). $\mathbb{S}^E$ links the free strain ($\boldsymbol{\varepsilon}^I_\mu$) in a region (the inclusion) of the infinite media to the total strain $\boldsymbol{\varepsilon}^I$ in

[4] Such as the magnetic walls effect, the effect of the non-uniformity of the exchange energy, of the magnetic field or of the stress tensor in the single crystal.

[5] It can be either simulated or measured thanks to X-rays diffraction or electron back scattering diffraction (EBSD) measurements.

[6] For the applications considered in this paper inclusions are taken spherical, assuming an isotropic distribution of the grains.

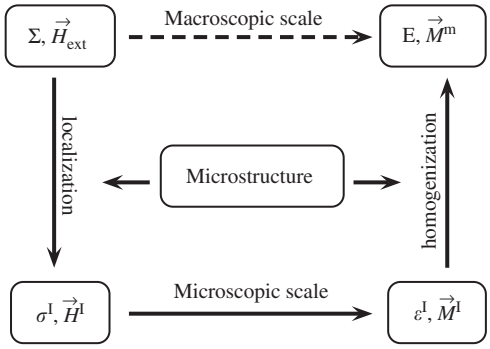


Fig. 1. Multiscale approach—principle.

this region

$$\boldsymbol{\varepsilon}^I = \mathbb{S}^E : \boldsymbol{\varepsilon}^I_\mu. \tag{24}$$

Hill's formula (Hill, 1965) is applied, giving the local stress $\boldsymbol{\sigma}^I$ (at the single crystal scale) as a function of the applied stress $\boldsymbol{\Sigma}$ (at the VER scale), the total strain $\boldsymbol{E}$ and the grain total strain $\boldsymbol{\varepsilon}^I$

$$\boldsymbol{\sigma}^I = \boldsymbol{\Sigma} + \mathbb{C}^* : (\boldsymbol{E} - \boldsymbol{\varepsilon}^I). \tag{25}$$

$\mathbb{C}^*$ is the so-called Hill's constraint tensor, defined according to the Eshelby solution for the inclusion problem

$$\mathbb{C}^* = \mathbb{C} : (\mathbb{S}^{E^{-1}} - \mathbb{I}), \tag{26}$$

$\mathbb{C}$ is the polycrystal stiffness tensor, and $\mathbb{I}$ the fourth order identity tensor.

Strains are then separated into elastic and magnetostrictive parts:

$$\begin{cases} \boldsymbol{E} = \boldsymbol{E}_e + \boldsymbol{E}_\mu = \mathbb{C}^{-1} : \boldsymbol{\Sigma} + \boldsymbol{E}_\mu, \\ \boldsymbol{\varepsilon}^I = \boldsymbol{\varepsilon}^I_e + \boldsymbol{\varepsilon}^I_\mu = \mathbb{C}^{I^{-1}} : \boldsymbol{\sigma}^I + \boldsymbol{\varepsilon}^I_\mu \end{cases} \tag{27}$$

leading to the relation

$$\boldsymbol{\sigma}^I = \mathbb{B}^I : \boldsymbol{\Sigma} + \mathbb{L}^*_{inc} : (\boldsymbol{E}_\mu - \boldsymbol{\varepsilon}^I_\mu). \tag{28}$$

The local stress is written as the sum of two terms:

- The first term depends on the macroscopic stress tensor $\boldsymbol{\Sigma}$ and on the stress concentration law. $\mathbb{B}^I$ is the stress concentration tensor in the purely elastic problem. It can be written

$$\mathbb{B}^I = \mathbb{C}^I : \mathbb{A}^I : \mathbb{C}^{-1} \quad \text{with } \mathbb{A}^I = (\mathbb{C}^I + \mathbb{C}^*)^{-1} : (\mathbb{C} + \mathbb{C}^*). \tag{29}$$

- The second term is linked to the elastic incompatibilities due to the existence of the free strain $\boldsymbol{\varepsilon}^I_\mu$ in the grain, and to the stiffness of the surrounding medium. $\boldsymbol{E}_\mu$ is the macroscopic magnetostriction strain. $\mathbb{L}^*_{inc}$ is defined by

$$\mathbb{L}^*_{inc} = \mathbb{C}^I : (\mathbb{C}^I + \mathbb{C}^*)^{-1} : \mathbb{C}^*. \tag{30}$$

The proposed expression for this incompatibility stress supposes that the overall behavior remains in the elastic domain.[7] Otherwise relaxation terms would have to be accounted for.[8]

A third term $\boldsymbol{\sigma}^I_{res}$ can be added in order to account for residual stresses associated to other incompatibility phenomena. These incompatibilities can be linked to plasticity, thermal or transformation strain. Eq. (28)

[7]This condition is verified for most of ferro and ferrimagnetic materials, for which magnetostriction magnitude is about $10^{-6}$–$10^{-4}$, and maximum elastic strain magnitude is about $10^{-3}$–$10^{-2}$.

[8]The approach would then join plasticity or phase transformation micro–macro modeling.

becomes

$$\boldsymbol{\sigma}^I = \mathbb{B}^I : \boldsymbol{\Sigma} + \mathbb{L}^*_{\text{inc}} : (\boldsymbol{E}_\mu - \boldsymbol{\varepsilon}^I_\mu) + \boldsymbol{\sigma}^I_{\mathbf{res}} \tag{31}$$

with

$$\frac{1}{V}\int_{\mathbf{VER}} \boldsymbol{\sigma}^I_{\mathbf{res}}\,\mathrm{d}V = \langle \boldsymbol{\sigma}^I_{\mathbf{res}} \rangle = \boldsymbol{O}. \tag{32}$$

It must be noticed that relation (28) (or (31)) is implicit, since $\boldsymbol{\varepsilon}^I_\mu$ and $\boldsymbol{E}_\mu$ are functions of $\boldsymbol{\sigma}^I$ and $\boldsymbol{\Sigma}$.

### 3.1.2. Definition of the local magnetic field

The aim of this step is to derive the local magnetic field $\vec{H}^{\mathbf{I}}$ from the external loading, postulating a given form for the function $h$ in relation (33)

$$\vec{H}^{\mathbf{I}} = h(\boldsymbol{\Sigma}, \vec{H}_{\mathbf{ext}}). \tag{33}$$

This equation is usually written (in electrotechnical engineering) in the form of relation (34)

$$\vec{H}^{\mathbf{I}} = \vec{H}_{\mathbf{ext}} + \vec{H}^{\mathbf{I}}_{\mathrm{d}}, \tag{34}$$

where the local perturbation of the macroscopic magnetic field is taken into account through the demagnetizing field $\vec{H}^{\mathbf{I}}_{\mathrm{d}}$. As we must verify

$$\frac{1}{V}\int_{\mathbf{VER}} \vec{H}^{\mathbf{I}}\,\mathrm{d}V = \langle \vec{H}^{\mathbf{I}} \rangle = \vec{H}_{\mathbf{ext}}, \tag{35}$$

we have

$$\frac{1}{V}\int_{\mathbf{VER}} \vec{H}^{\mathbf{I}}_{\mathrm{d}}\,\mathrm{d}V = \langle \vec{H}^{\mathbf{I}}_{\mathrm{d}} \rangle = \vec{0}. \tag{36}$$

Assuming that the mean values for the magnetization and the magnetic fields are sufficient to define the magnetic state of a grain, the demagnetizing field is written

$$\vec{H}^{\mathbf{I}}_{\mathrm{d}} = \boldsymbol{K}_{\mathrm{d}}(\vec{M}^{\mathbf{m}} - \vec{M}^{\mathbf{I}}) \tag{37}$$

with $\vec{M}^{\mathbf{m}}$ the mean magnetization in the material, $\vec{M}^{\mathbf{I}}$ the mean magnetization for the considered grain and $\boldsymbol{K}_{\mathrm{d}}$ a second order operator.

In the case of stress independent linear isotropic magnetic behavior, and spherical inclusions, the tensor $\boldsymbol{K}_{\mathrm{d}}$ can be replaced by a scalar value $N_{\mathrm{c}}$ (see Appendix C).

$$N_{\mathrm{c}} = \frac{1}{3 + 2\chi^{\mathbf{m}}}, \quad \chi^{\mathbf{m}} \text{ is the equivalent media susceptibility.} \tag{38}$$

Herein, as a first approximation, we choose to extend this relation to anisotropic non-linear magnetic behavior. We use a variable value of $N_{\mathrm{c}}$ computed from the value of $\chi^{\mathbf{m}}$ recalculated at each step of the iterative scheme (secant definition)

$$\chi^{\mathbf{m}} = \frac{\|\vec{M}^{\mathbf{m}}\|}{\|\vec{H}_{\mathbf{ext}}\|}. \tag{39}$$

The localization law[9] (Eq. (34)) is then written

$$\vec{H}^{\mathbf{I}} = \vec{H}_{\mathbf{ext}} + \frac{1}{3 + 2\chi^{\mathbf{m}}}(\vec{M}^{\mathbf{m}} - \vec{M}^{\mathbf{I}}). \tag{40}$$

[9]The adopted modeling is similar to the secant approach used in the framework of micro–macro modeling of plasticity, and exhibits the same limitations, particularly for high levels of non-linearity (Gilormini, 1995).

### 3.2. Local behavior

Local behavior is defined according to Section 2. The local loading—applied to a grain—being known, the local behavior law can be applied, and the grain response (magnetization and strain) deduced.

### 3.3. Homogenization

The last step in the micro–macro modeling is the homogenization step to go back to the macro-scale. We define:

$$\begin{cases} \vec{M}^{\mathbf{m}} = \dfrac{1}{V}\displaystyle\int_{\mathbf{VER}} \vec{M}\,\mathrm{d}V = \langle \vec{M}^{\mathbf{I}} \rangle, \\ \boldsymbol{E} = \dfrac{1}{V}\displaystyle\int_{\mathbf{VER}} \boldsymbol{\varepsilon}\,\mathrm{d}V = \langle \boldsymbol{\varepsilon}^{I} \rangle. \end{cases} \tag{41}$$

As the scheme is self-consistent, an iterative procedure has to be built up. The calculation is then done until convergence.

The resolution of a complete coupled magneto-elastic problem requires a numerical implementation of the modeling, including discrete ODF data. An example is given on Section 4.2 in the case of isotropic polycrystalline iron. Nevertheless, analytical solutions can be found in the case of isotropic polycrystals, using similar ideas. The particular case of magnetic saturation, leading to an usual thermo-elastic problem, is treated in Appendix D.

## 4. Modeling results

### 4.1. Single crystals

We compare in this section the results of modeling to the experimental data obtained by Webster (1925a,b) for pure iron single crystals.

Low fields measurements give the necessary data to identify the parameter $A_s$. The initial susceptibility of the single crystal is approximatively estimated thanks to the $\langle 1\,0\,0 \rangle$ magnetization curve

$$\chi^0_{\mathbf{exp}} \backsimeq 2000 \quad \text{leading to } A_s = 1.6 \times 10^{-3}\,\mathrm{m^3\,J^{-1}}. \tag{42}$$

This result is obviously approximative since it is based only on the behavior along the $\langle 1\,0\,0 \rangle$ axis. Experimental data indicate that the initial susceptibility in other directions is a little lower, in disaccordance with our initial hypotheses. The material constants used are defined in Table 1.

Fig. 2(a) (resp. 2(b)) shows the magnetization (resp. the magnetostriction strain) measured in the direction parallel to the magnetic field, when magnetic field is applied along a $\langle 1\,0\,0 \rangle$, $\langle 1\,1\,0 \rangle$ or $\langle 1\,1\,1 \rangle$ axis of the single crystal. We observe a very good agreement between numerical and experimental results, both for magnetic and magnetostrictive behaviors. Strong non-linearity and anisotropy are well reproduced.

### 4.2. Polycrystals

In the case of polycrystals, the choice of a discrete modeling seems quite natural as the texture data (ODF) are often available under the form of discrete data.

Table 1
Pure iron single crystal characteristics—bibliographic data

| Constant | Value | Reference |
|---|---|---|
| $M_s$ | $1.71 \times 10^6\,\mathrm{A/m}$ | Bozorth (1951), Cullity (1972), Jiles (1991) |
| $(K_1; K_2)$ | $(42.7; 15)\,\mathrm{kJ/m^3}$ | Bozorth (1951) |
| $(\lambda_{100}; \lambda_{111})$ | $(21; -21)10^{-6}$ | Cullity (1972), Jiles (1991) |
| $(C_{11}, C_{12}, C_{44})$ | (238;142;232) GPa | McClintock and Argon (1966) |

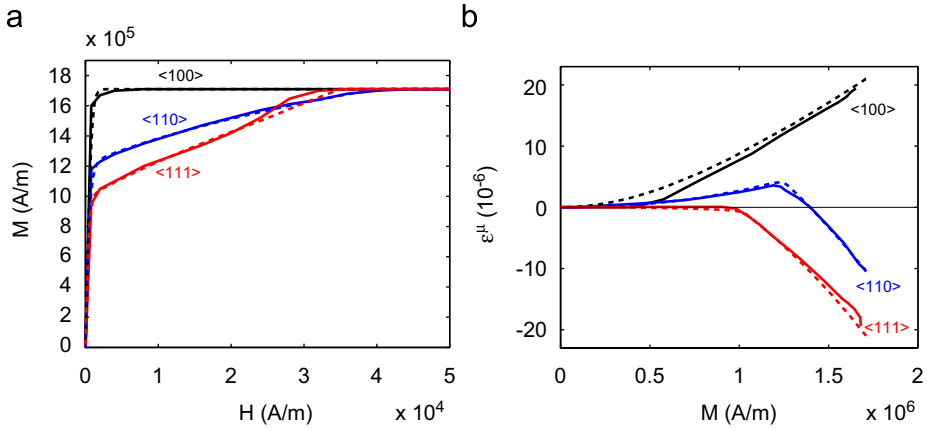


Fig. 2. Pure iron single crystal behaviour. Experimental data (Webster, 1925a,b) (line) and numerical results (dashed line): (a) magnetization curve; (b) magnetostrictive curve.

Modeling results are illustrated in the case of isotropic pure iron polycrystal. The material parameters used are listed in Table 1. They are relative to the single crystal, except $A_s$. The experimental results of Kuruzar and Cullity (1971) allow to define the parameter $A_s$ in the case of iron: $A_s = 2 \times 10^{-3}\,\mathrm{m^3\,J^{-1}}$.

The first possible way to describe the crystallographic orientation distribution function is to choose of a random orientation for each grain. This choice leads to a great uncertainty on the results obtained for the magnetostriction strain as it is illustrated in Fig. 3.[10]

For a number of 100 orientations, the obtained value of the saturation magnetostriction strain lies in a wide band—150% around the theoretical value. This dispersion (defined with a six standard deviation width) is very slowly decreasing when increasing the number of orientations. A 1000 orientations distribution function does not allow to define the magnetostriction in a band thinner than 50% around the theoretical value. The mean value over the 200 random distribution functions leads approximatively to the correct value for the saturation strain, whatever the—reasonable—number of orientations chosen. A solution to get precise results would be to define a great number of random distribution functions, and to define the mean value for the obtained results. This solution appears to be expensive in terms of computation time.

Another choice, already used by Buiron (2000), is to build a regular zoning in the space of possible orientations. Each crystal is defined by three Euler angles ($\varphi_1$, $\psi$, $\varphi_2$) following Bunge notation. Each angle takes values regularly distributed in their variation domain, following Table 2.

The number of values taken in each space domain gives the precision of the texture isotropy. Limitation is still linked to the number of orientations which has to be low in order to get reasonable computation times. One possible ODF is made of 546 different orientations. The corresponding poles figures are given in Fig. 4.

This regular distribution exhibits a weak but obvious isotropic transverse symmetry. As shown in Fig. 3, the Reuss magnetostriction saturation strain is a good indicator of anisotropy for a given texture. It has been calculated for the 546 orientations texture, considering a great number (2000) of random directions of the magnetic field. The obtained mean value is $-4.18 \times 10^{-6}$, which is very near from the theoretical value ($-4.20 \times 10^{-6}$). Standard deviation reaches $S = 6.8 \times 10^{-8}$, so that the dispersion reported in Fig. 3 is associated to an error bar of $\pm 0.05$. This dispersion corresponds to a number of random orientations more than 5000. As a conclusion, the constructed data file leads to quasi-isotropic behavior and will be kept to describe isotropic materials.

The multiscale approach presented in Section 3 has been applied using this "isotropic" texture data, and the iron single crystal characteristics (Table 1).

[10]The sensibility of the results to the texture data is highly dependent on the contrast between the constants $\lambda_{100}$ and $\lambda_{111}$.

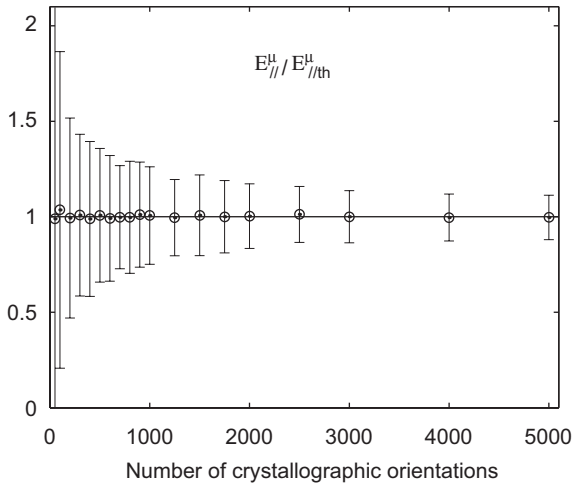


Fig. 3. Dispersion obtained—for 200 random orientation distribution functions—on the Reuss estimate value for the saturation magnetostriction strain, depending on the number of orientations considered for this distribution function.

Table 2
Values chosen for the Euler angle for the "isotropic" texture

| Variable | Domain | Number of values |
|---|---|---|
| $\varphi_1$ | $[0, 2\pi]$ | 13 |
| $\cos\psi$ | $[0, 1]$ | 7 |
| $\varphi_2$ | $[0, 2\pi]$ | 6 |

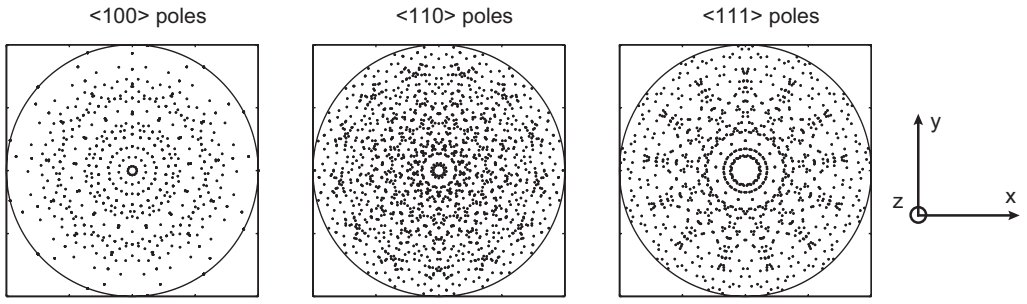


Fig. 4. Pole figures for the "isotropic" polycrystal obtained by regular zoning of the crystallographic orientations space (stereographic projection).

### 4.2.1. Elastic behavior

Self-consistent and Voigt estimates for the shear modulus associated to this (discrete) virtual material have been calculated:

$$\mu^{\mathbf{eff}\,\mathbf{SC}} \simeq 82.1\,\mathrm{GPa} \quad \text{and} \quad \mu^{\mathbf{eff}\,\mathbf{V}} \simeq 88.8\,\mathrm{GPa}. \tag{43}$$

The calculation of the corresponding theoretical values is presented in Appendix D. If no more significant figure is needed, the results given by the discrete approach are exactly the same than the analytical ones (Table D.1). From that observation, we can conclude that the 546 orientations distribution allows an accurate description of the elastic behavior of an isotropic polycrystal.

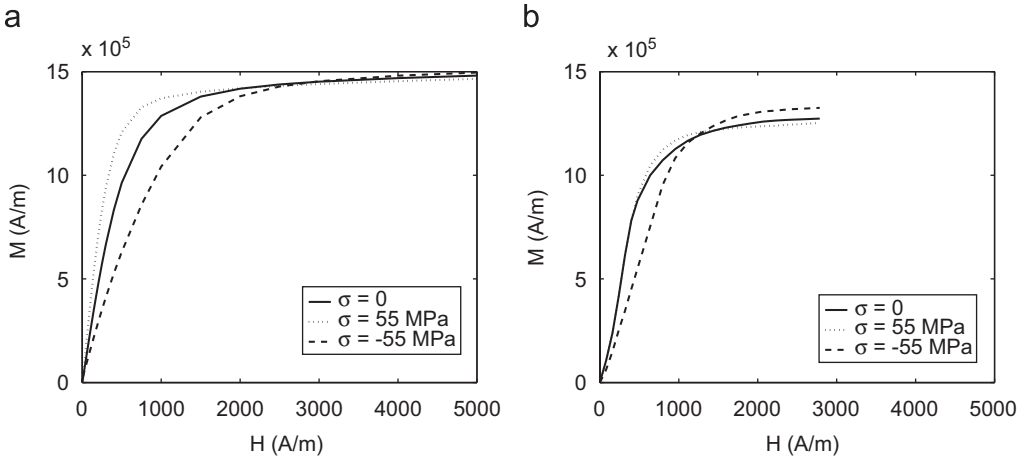


Fig. 5. Effect of uniaxial stress on the magnetization curve: (a) numerical results; (b) experimental results (Kuruzar and Cullity, 1971).

#### 4.2.2. Saturation magnetostriction strain

The saturation magnetostriction strain is obtained using a very high applied magnetic field along the $\vec{z}$ axis.[11] Self-consistent and Reuss estimates have been calculated

$$\boldsymbol{E}^{\|546}_{\mu_{\mathbf{SC}}} = -8.95 \times 10^{-6} \quad \text{and} \quad \boldsymbol{E}^{\|546}_{\mu_{\mathbf{R}}} = -4.41 \times 10^{-6}. \tag{44}$$

These results are close to the analytical ones presented in Table D.2, but the agreement is less accurate than for elastic properties: magnetostrictive properties of polycrystals are much more texture dependent than elastic properties.

#### 4.2.3. Magnetic behavior

The multiscale modeling allows to predict both the magnetic and magnetostrictive behaviors of the material for different values of the external field and stress. In this case, no analytical solution are available, since linear behavior and field homogeneity assumptions cannot be made anymore. Results obtained for the anhysteretic magnetization curves are shown in Fig. 5(a) for several levels of uniaxial applied stress. Fig. 5(b) shows corresponding experimental results obtained by Kuruzar and Cullity (1971) for pure polycrystalline iron (see also Cullity, 1972).

Comparison between experimental and numerical results shows that the multiscale model seems to describe correctly the effect of an applied stress. For low levels of magnetic field, a tensile stress increases the magnetic susceptibility whereas a compression decreases it, in a stronger way. This effect is inversed for higher levels of the applied magnetic field (Villari reversal), and the modeling reproduces it. The crossover between the magnetization curves for different stress levels is usually explained by an inversion of the evolution of the magnetostriction strain, introducing a change in the sense of variation for the magneto-elastic energy. This point is directly related to the magnetization rotation mechanism.

Nevertheless, the modeling tends to overestimate the magnetic behavior, and the crossover point between the different magnetization curves is obtained for higher magnetic field levels. However, the quantitative comparison is hazardous, since the results of Kuruzar and Cullity (1971) are first magnetization curves (meaning hysteretic measurements). Moreover the material used by Kuruzar and Cullity (1971) is supposed to be isotropic, but the grain orientation distribution is actually unknown.

#### 4.2.4. Magnetostrictive behavior

Experimental observations (Fig. 6(b)) show that the magnetostriction strain first increases with the applied field and then decreases until a saturation point is reached. The effect of the magnetic field on the strain is

[11] $\vec{z}$ is the direction normal to the plane of poles figures.

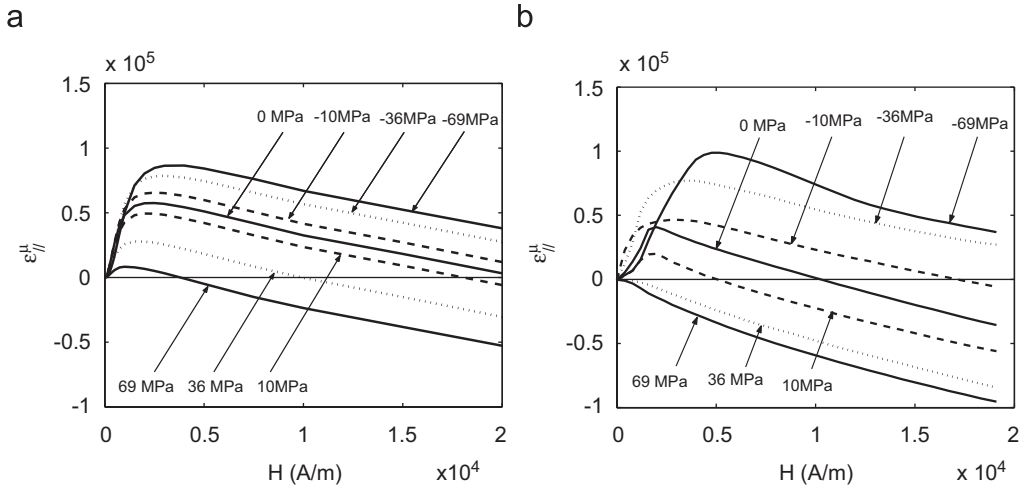


Fig. 6. Effect of uniaxial stress on the magnetostriction curve: (a) numerical results; (b) experimental results (Kuruzar and Cullity, 1971).

correctly reproduced by the modeling[12] (Fig. 6(a)), qualitatively concerning the general level, and quantitatively concerning the slopes of the curves. The effect of uniaxial stress on the strain level is correctly reproduced, even if the observed amplitude for the strain variations is higher than the predicted one.

## 5. Conclusion

In this paper, a model for the reversible magneto-mechanical behavior of magnetic materials, accounting for 3D magnetization and multiaxial stress state has been presented.

The multiscale model can be described as a simplified micro-magnetic model. Several scales are chosen to define the magneto-elastic behavior, leading to a multiscale calculation strategy. The first scale is the magnetic domains scale, at which the magnetization can be considered as homogeneous. The next scale is the single crystal scale where elastic properties are homogeneous. The last scale is the RVE scale, which is large enough to define the average material behavior and properties. Calculation of whole magneto-elastic behavior requires the use of a single crystal modeling.

Potential energy is written at domain scale considering three energetic terms: magnetostatic energy, magnetocrystalline energy and elastic energy. The internal variables are volumetric fraction and magnetization orientation of each magnetic domain family: it means 18 internal variables for crystals with $\langle 1\,0\,0\rangle$ easy directions and 24 for crystal with $\langle 1\,1\,1\rangle$ easy directions. Each internal variable is calculated thanks to a two steps procedure: energetic minimization for orientations calculation and explicit Boltzmann formulation for the calculation of volumetric fractions. Single crystal magnetization and magnetostriction are calculated thanks to averaging operations over the domains.

Specific localization and homogenization procedures from RVE to grain scale are nevertheless required for local magnetic and mechanical fields calculation. Secant approach is used for magnetic behavior, which is strongly non-linear; elastic behavior remains linear and convergence is easily reached.

The multiscale model is able to predict: (1) magnetic behavior; (2) elastic behavior; (3) influence of multiaxial stress state on magnetization; (4) magnetostrictive behavior; (5) influence of multiaxial stress state on the magnetostrictive behavior; isotropic material as well as strongly textured material (Hubert et al., 2003) can be considered. Comparisons to experimental data obtained from iron-silicon sheets (Daniel et al., 2003), or isotropic ferrimagnetic NiZn ferrite (Vieille et al., 2004; Daniel et al., 2007) are conclusive.

The main shortcomings of the model are first that magnetic and mechanical fields are considered homogeneous within a single crystal; second that domain walls are not taken into account (domain walls lead

[12]For which the reference strain is put to zero at zero magnetic field, whatever the stress level. It is imposed by the presentation of the experimental data.

to an increase of energy due to exchange energy contribution). A third important limitation is that the domain configuration is only seen through volumetric fractions, which is insufficient when considering the importance of the domains distribution on the local demagnetizing fields. Finally, surface effect has to be considered when the grain size is comparable to the thickness of material (Hubert et al., 2003; Daniel et al., 2004).

Future developments will consist in introducing residual stresses effects such as plasticity or thermal stresses, and dynamic and dissipative phenomena.

## Appendix A

### A.1. Definition of the elastic energy

The elastic energy for a domain is written

$$W_\sigma = \tfrac{1}{2}\boldsymbol{\varepsilon}_e^\alpha : \mathbb{C}^I : \boldsymbol{\varepsilon}_e^\alpha = \tfrac{1}{2}\boldsymbol{\sigma}^\alpha : \mathbb{C}^{I^{-1}} : \boldsymbol{\sigma}^\alpha. \tag{A.1}$$

Several cases can be considered:

- If the stress is supposed uniform over the grain, $\boldsymbol{\sigma}^\alpha = \boldsymbol{\sigma}^I$, and then

$$W_\sigma^\alpha = \tfrac{1}{2}\boldsymbol{\sigma}^I : \mathbb{C}^{I^{-1}} : \boldsymbol{\sigma}^I. \tag{A.2}$$

  This term is uniform over a single crystal, no magneto-elastic interaction appears.
- If the strain is supposed uniform over the grain, $\boldsymbol{\varepsilon}^\alpha = \boldsymbol{\varepsilon}^I$, and then

$$\begin{aligned} W_\sigma^\alpha &= \tfrac{1}{2}\boldsymbol{\varepsilon}_e^\alpha : \mathbb{C}^I : \boldsymbol{\varepsilon}_e^\alpha \\ &= \tfrac{1}{2}(\boldsymbol{\varepsilon}^\alpha - \boldsymbol{\varepsilon}_\mu^\alpha) : \mathbb{C}^I : (\boldsymbol{\varepsilon}^\alpha - \boldsymbol{\varepsilon}_\mu^\alpha) \\ &= \tfrac{1}{2}\boldsymbol{\varepsilon}^\alpha : \mathbb{C}^I : \boldsymbol{\varepsilon}^\alpha + \tfrac{1}{2}\boldsymbol{\varepsilon}_\mu^\alpha : \mathbb{C}^I : \boldsymbol{\varepsilon}_\mu^\alpha - \boldsymbol{\varepsilon}_\mu^\alpha : \mathbb{C}^I : \boldsymbol{\varepsilon}^\alpha \\ &= \tfrac{1}{2}\boldsymbol{\varepsilon}^I : \mathbb{C}^I : \boldsymbol{\varepsilon}^I + \tfrac{1}{2}\boldsymbol{\varepsilon}_\mu^\alpha : \mathbb{C}^I : \boldsymbol{\varepsilon}_\mu^\alpha - \boldsymbol{\varepsilon}_\mu^\alpha : \mathbb{C}^I : (\boldsymbol{\varepsilon}_\mu^I + \boldsymbol{\varepsilon}_e^I) \\ &= \tfrac{1}{2}\boldsymbol{\varepsilon}^I : \mathbb{C}^I : \boldsymbol{\varepsilon}^I + \tfrac{1}{2}\boldsymbol{\varepsilon}_\mu^\alpha : \mathbb{C}^I : \boldsymbol{\varepsilon}_\mu^\alpha - \boldsymbol{\varepsilon}_\mu^\alpha : \mathbb{C}^I : \boldsymbol{\varepsilon}_\mu^I - \boldsymbol{\sigma}^I : \boldsymbol{\varepsilon}_\mu^\alpha. \end{aligned} \tag{A.3}$$

  A magneto-elastic interaction appears. If we neglect the second order terms (considering that $\mathbb{C}^I : \boldsymbol{\varepsilon}_\mu^\alpha$ and $\mathbb{C}^I : \boldsymbol{\varepsilon}_\mu^I$ are much smaller than $\boldsymbol{\sigma}^I$), we get the usual magneto-elastic interaction term (Hubert and Schäfer, 1998)

$$W_\sigma^\alpha = W_\sigma^o - \boldsymbol{\sigma}^I : \boldsymbol{\varepsilon}_\mu^\alpha, \tag{A.4}$$

  $W_\sigma^o$ being a constant over the grain, whatever the magnetization state

$$W_\sigma^o = \tfrac{1}{2}\boldsymbol{\varepsilon}^I : \mathbb{C}^I : \boldsymbol{\varepsilon}^I. \tag{A.5}$$

- Hill's approach can also be used (Hill, 1965) to treat an intermediate situation. Hill's formula is applied, giving the local stress $\boldsymbol{\sigma}^\alpha$ as a function of the applied stress $\boldsymbol{\sigma}^I$ (at the single crystal scale), the single crystal total strain $\boldsymbol{\varepsilon}^I$ and the domain total strain $\boldsymbol{\varepsilon}^\alpha$

$$\boldsymbol{\sigma}^\alpha = \boldsymbol{\sigma}^I + \mathbb{C}^* : (\boldsymbol{\varepsilon}^I - \boldsymbol{\varepsilon}^\alpha). \tag{A.6}$$

  $\mathbb{C}^*$ is the so-called Hill's constraint tensor, defined after the Eshelby solution for the inclusion problem (Eshelby, 1957)

$$\mathbb{C}^* = \mathbb{C}^I : (\mathbb{S}^{E^{-1}} - \mathbb{I}). \tag{A.7}$$

  $\mathbb{S}^E$ is the so-called Eshelby tensor, and $\mathbb{I}$ the fourth order identity tensor. The strain is then separated into elastic and magnetostrictive parts

$$\begin{cases} \boldsymbol{\varepsilon}^I = \boldsymbol{\varepsilon}_e^I + \boldsymbol{\varepsilon}_\mu^I = \mathbb{C}^{I^{-1}} : \boldsymbol{\sigma}^I + \boldsymbol{\varepsilon}_\mu^I, \\ \boldsymbol{\varepsilon}^\alpha = \boldsymbol{\varepsilon}_e^\alpha + \boldsymbol{\varepsilon}_\mu^\alpha = \mathbb{C}^{I^{-1}} : \boldsymbol{\sigma}^\alpha + \boldsymbol{\varepsilon}_\mu^\alpha \end{cases} \tag{A.8}$$

leading to the relation

$$\boldsymbol{\sigma}^{\alpha} = \boldsymbol{\sigma}^{I} + \mathbb{C}^{I} : (\mathbb{I} - \mathbb{S}^{\mathrm{E}}) : (\boldsymbol{\varepsilon}_{\mu}^{I} - \boldsymbol{\varepsilon}_{\mu}^{\alpha}). \tag{A.9}$$

The elastic energy can now be written

$$\begin{aligned} W_{\sigma}^{\alpha} &= \tfrac{1}{2}\boldsymbol{\sigma}^{\alpha} : \mathbb{C}^{I^{-1}} : \boldsymbol{\sigma}^{\alpha} \\ &= \tfrac{1}{2}\boldsymbol{\sigma}^{I} : \mathbb{C}^{I^{-1}} : \boldsymbol{\sigma}^{I} + \tfrac{1}{2}(\boldsymbol{\varepsilon}_{\mu}^{I} - \boldsymbol{\varepsilon}_{\mu}^{\alpha}) : \mathbb{C}^{I} : (\mathbb{I} - \mathbb{S}^{\mathrm{E}}) : (\boldsymbol{\varepsilon}_{\mu}^{I} - \boldsymbol{\varepsilon}_{\mu}^{\alpha}) + \boldsymbol{\sigma}^{I} : (\mathbb{I} - \mathbb{S}^{\mathrm{E}}) : (\boldsymbol{\varepsilon}_{\mu}^{I} - \boldsymbol{\varepsilon}_{\mu}^{\alpha}) \\ &= W_{\sigma}^{\mathrm{o}} - \boldsymbol{\sigma}^{I} : (\mathbb{I} - \mathbb{S}^{\mathrm{E}}) : \boldsymbol{\varepsilon}_{\mu}^{\alpha} + \tfrac{1}{2}\boldsymbol{\varepsilon}_{\mu}^{\alpha} : \mathbb{C}^{I} : (\mathbb{I} - \mathbb{S}^{\mathrm{E}}) : \boldsymbol{\varepsilon}_{\mu}^{\alpha} - \boldsymbol{\varepsilon}_{\mu}^{I} : \mathbb{C}^{I} : (\mathbb{I} - \mathbb{S}^{\mathrm{E}}) : \boldsymbol{\varepsilon}_{\mu}^{\alpha}. \end{aligned} \tag{A.10}$$

If $\mathbb{S}^{\mathrm{E}}$ is supposed constant, $W_{\sigma}^{\mathrm{o}}$ is a constant over the grain, whatever the magnetization state

$$W_{\sigma}^{\mathrm{o}} = \tfrac{1}{2}\boldsymbol{\sigma}^{I} : \mathbb{C}^{I^{-1}} : \boldsymbol{\sigma}^{I} + \tfrac{1}{2}\boldsymbol{\varepsilon}_{\mu}^{I} : \mathbb{C}^{I} : (\mathbb{I} - \mathbb{S}^{\mathrm{E}}) : \boldsymbol{\varepsilon}_{\mu}^{I} + \boldsymbol{\sigma}^{I} : (\mathbb{I} - \mathbb{S}^{\mathrm{E}}) : \boldsymbol{\varepsilon}_{\mu}^{I}. \tag{A.11}$$

Only the non-uniform part of $W_{\sigma}^{\alpha}$ plays a role in the energetic equilibrium. The latter assumptions leads to intermediate estimates, but is associated to more complicated calculations (to get the Eshelby tensor).

## Appendix B. A simplified approach for the identification of $A_{\mathrm{s}}$ parameter

### *B.1. Single crystal*

#### *B.1.1. A simplified approach*

When the description of the magnetic behavior is restricted to low fields and stress states, the rotation mechanism is usually neglected. A way to define the validity range of such an hypothesis is to consider the so-called "anisotropy" field (Chikazumi, 1997). The anisotropy magnetic and stress fields are defined by Eq. (B.1)

$$H_K = \frac{K_1}{\mu_0 M_{\mathrm{s}}} \quad \text{and} \quad \sigma_K = \frac{K_1}{\lambda_S}. \tag{B.1}$$

The rotation mechanism can be neglected until magnetic field or stress levels stand far from the anisotropy fields.[13]

Under these conditions, the potential energy of a domain can be written

$$W^{\alpha} = -\mu_0 \vec{M}^{\alpha}.\vec{H}^{\mathbf{I}}. \tag{B.2}$$

The volumetric fraction of each domain family is still defined by Eq. (18). We note, for further simplifications

$$\begin{cases} \vec{M}^{\alpha} = M_{\mathrm{s}}\vec{\gamma}^{\alpha}, \\ H = \|\vec{H}^{\mathbf{I}}\|, \\ S = \sum\limits_{\alpha} \exp(-A_{\mathrm{s}}.W^{\alpha}), \\ K = A_{\mathrm{s}}\mu_0 H M_{\mathrm{s}}. \end{cases} \tag{B.3}$$

In the crystallographic frame, using spherical coordinates for the magnetic field ($\vec{H}^{\mathbf{I}} = H[\sin\varphi\cos\theta, \sin\varphi\sin\theta, \cos\varphi]$), the potential energy of the domain families can be explicitly written, and $S$ is deduced:

$$S = 2(\cosh(K\sin\varphi\cos\theta) + \cosh(K\sin\varphi\sin\theta) + \cosh(K\cos\varphi)). \tag{B.4}$$

The single crystal magnetization is given by

$$\vec{M}^{\mathbf{I}} = \frac{2M_{\mathrm{s}}}{S} \begin{vmatrix} \sinh(K\sin\varphi\cos\theta), \\ \sinh(K\sin\varphi\sin\theta), \\ \sinh(K\cos\varphi). \end{vmatrix} \tag{B.5}$$

[13] $H_K$ (resp. $\sigma_K$) corresponds to a situation when the magnetic energy (resp. the elastic energy) totally compensate the magneto-crystalline energy. In the case of iron $H_K \simeq 20\,\mathrm{kA/m}$ and $\sigma_K \simeq 2\,\mathrm{GPa}$. In the case of nickel $H_K \simeq 5.5\,\mathrm{kA/m}$ and $\sigma_K \simeq 73\,\mathrm{MPa}$.

The single crystal magnetostriction can also be written

$$\varepsilon_{\mu}^{I}=\frac{\lambda_{100}}{S}\begin{pmatrix} 2\cosh(K\sin\varphi\cos\theta) & 0 & 0 \\ -(\cosh(K\sin\varphi\sin\theta)+\cosh(K\cos\varphi)) & & \\ 0 & 2\cosh(K\sin\varphi\sin\theta) & 0 \\ & -(\cosh(K\sin\varphi\cos\theta)+\cosh(K\cos\varphi)) & \\ 0 & 0 & 2\cosh(K\cos\varphi) \\ & & -(\cosh(K\sin\varphi\cos\theta)+\cosh(K\sin\varphi\sin\theta)) \end{pmatrix}. \tag{B.6}$$

These relations can be considered as a simplified modeling for the magnetization and magnetostriction of a single crystal as a function of the applied magnetic field. This modeling is anisotropic, as coordinates $\theta$ and $\varphi$ are involved. Its validity area is however very tiny as it does not account for rotation mechanisms nor effect of an applied stress.

Experimental data obtained by Webster (1925a) for pure iron are reported in Fig. B.1 and compared to modeling results. Since the modeling does not account for the out of easy directions rotation mechanism, the simplified model will not be able to predict a saturation state if the applied field is oriented along a $\langle 1\,1\,0\rangle$ or $\langle 1\,1\,1\rangle$ direction, or more generally in a direction that is not an easy magnetization direction.

### *B.1.2. Initial susceptibility definition*

The assumptions made in the previous paragraph do not allow to use this modeling for high magnetic fields. But interesting informations can be obtained in the vicinity of a null applied field. We can observe the evolution of the magnetization in the vicinity of zero by calculating its derivative with $H$. After calculation, we obtain

$$\left.\frac{\partial\vec{M}^{\mathbf{I}}}{\partial H}\right|_{H=0}=\frac{\mu_0 A_s M_s^2}{3}\frac{\vec{H}}{H}. \tag{B.7}$$

Near the origin, the magnetization rises and keeps its direction parallel to the applied magnetic field. The material initial susceptibility, defined as the slope at the origin of the magnetization curve, can thus be written

$$\chi^0=\tfrac{1}{3}A_s\mu_0 M_s^2. \tag{B.8}$$

The constant $A_s$ can therefore be identified using a single magnetization curve of the crystal

$$A_s=\frac{3\chi^0}{\mu_0 M_s^2}. \tag{B.9}$$

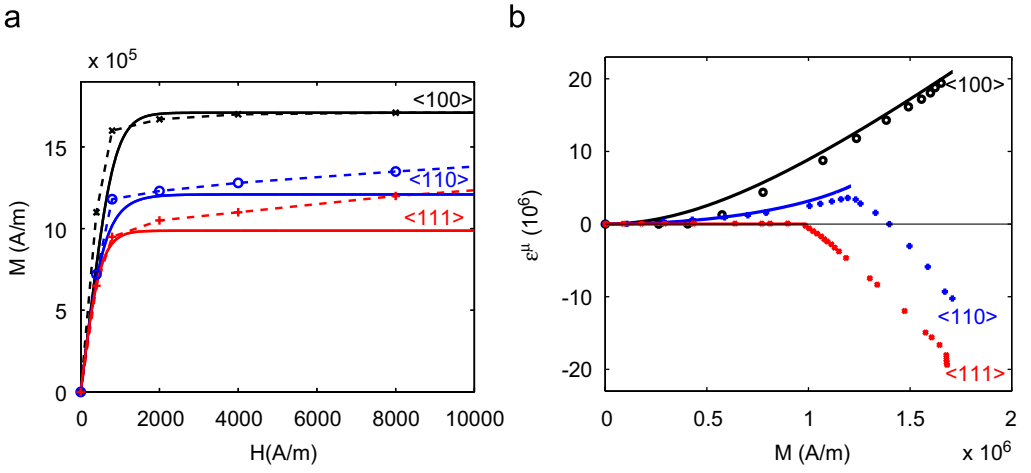


Fig. B.1. Simplified modeling for the iron single crystal behavior: experimental data (Webser, 1925a,b) (lines) and numerical results (dots): (a) magnetization; (b) magnetostriction.

The proposed simplified modeling is isotropic near the origin, as the predicted initial susceptibility is the same for every direction of the single crystal, and the predicted magnetization is parallel to the applied magnetic field. The anisotropic character of the behavior only appears for higher magnetic fields.

### B.2. Polycrystals

#### B.2.1. A simplified approach

Let us consider an—ideal—unstressed bulk isotropic ferromagnetic material. The polycrystal microstructure is seen as an assembly of magnetic domains. By opposition to the single crystal, all the possible orientations in space are considered equiprobable, and the domains are randomly distributed. The macroscopic behavior is then isotropic.

We will estimate the polycrystal behavior by considering that a polycrystal is a single crystal for which all space directions are easy magnetization directions. For each domain $\alpha$, we can write

$$\vec{M}^{\alpha} = M_s \vec{\gamma}^{\alpha}. \tag{B.10}$$

The macroscopic magnetization is written

$$\vec{M} = \frac{1}{V}\int_V \vec{M}^{\alpha}\,\mathrm{d}V = M_s \int_{\alpha} f^{\alpha}\vec{\gamma}^{\alpha}\,\mathrm{d}\alpha. \tag{B.11}$$

Using the same notations and simplifications than in Section B.1, we define

$$f^{\alpha} = \frac{1}{S}\exp(K\cos\varphi) \tag{B.12}$$

with

$$S = \int_{\alpha} \exp(-A_s W^{\alpha})\,\mathrm{d}\alpha = \int_{\alpha} \exp(A_s \mu_0 M_s \vec{\gamma}^{\alpha}.\vec{H})\,\mathrm{d}\alpha. \tag{B.13}$$

If the magnetic field is aligned with the $\vec{z}$ direction ($\vec{H} = H[0,0,1]$), we get

$$S = \frac{4\pi \sinh K}{K} \tag{B.14}$$

so that

$$\vec{M} = M_s \frac{K\cosh(K) - \sinh(K)}{K\sinh(K)}\vec{z}. \tag{B.15}$$

#### B.2.2. Initial susceptibility definition

This macroscopic modeling does not take into account the magnetization rotation mechanism, and thus, its validity domain is limited to the low applied fields area. Furthermore, only unstressed material has been considered. An interesting quantity to be studied is the initial susceptibility $\chi^0$

$$\chi^0 = \left.\frac{\partial M_z}{\partial H}\right|_{H=0}. \tag{B.16}$$

We get

$$\frac{\partial M_z}{\partial H} = A_s \mu_0 M_s^2 \frac{\sinh^2(K) - K^2}{K^2\sinh^2(K)} \tag{B.17}$$

leading to, for $K = 0$

$$\chi^0 = \tfrac{1}{3} A_s \mu_0 M_s^2. \tag{B.18}$$

We obtain for a polycrystal, the same definition for $\chi^0$ as in the case of a single crystal. This point results from the fact that, in the simplified approach, the polycrystal is seen as a single crystal with an infinity of easy magnetization directions (all directions of space being easy magnetization directions). A way to identify the value for $A_s$ is to get the initial slope of the macroscopic anhysteretic magnetization curve, and to deduce the

value of $A_s$ from it

$$A_s = \frac{3\chi^0}{\mu_0 M_s^2}. \tag{B.19}$$

*B.3. Simplified modeling for the anhysteretic magnetostriction curve*

As for the magnetization curve, it is possible to define a simplified modeling for the magnetostriction curve. This approach neglects the magnetization rotation phenomenon, so that the extreme value for magnetostriction is identical to its saturation value.

The definition of the volumetric fractions given by Eq. (B.12) is still correct. The single crystal magnetostriction strain can be written, considering that the stress is uniformly zero within the material:

$$\boldsymbol{E}_\mu = \int_\alpha f^\alpha \boldsymbol{\varepsilon}_\mu^{\alpha\prime} \, \mathrm{d}\alpha. \tag{B.20}$$

The definition of $\boldsymbol{\varepsilon}_\mu^{\alpha\prime}$ has to be specified. This definition is different from the usual definition of the magnetostriction strain in a domain (given in Eq. (D.9)) in order to account for the fact that crystallographic data has been totally neglected in this simplified modeling. $\boldsymbol{\varepsilon}_\mu^{\alpha\prime}$ must satisfy the two following properties:

- When the applied field is zero, the macroscopic magnetostriction strain is zero.
- When saturation is reached, $\boldsymbol{E}_\mu$ reaches a maximum value $\mathbf{E}_{\mu_{\mathbf{max}}}$ (that can be taken from Appendix D).

Considering the saturation state, for which the volumetric fraction of a domain—the one whose magnetization is parallel to the applied field—becomes 1, and the others become zero, we get

$$\boldsymbol{\varepsilon}_\mu^{\alpha\prime} = \mathbf{E}_{\mu_{\mathbf{max}}}. \tag{B.21}$$

As it is shown in Appendix D, this value can be written

$$\boldsymbol{\varepsilon}_\mu^{\alpha\prime} = \frac{2}{5}\lambda_{100} k^{\mathbf{a}} \begin{pmatrix} 1 & 0 & 0 \\ 0 & -\frac{1}{2} & 0 \\ 0 & 0 & -\frac{1}{2} \end{pmatrix}. \tag{B.22}$$

This strain tensor, initially written in the macroscopic frame, becomes the strain tensor of each domain family, in their own local frame.

The magnetostriction strain component $\mathbf{E}_{\mu_{zz}}$, parallel to the magnetic field can then be written

$$\mathbf{E}_{\mu_{zz}} = \int_\alpha f^\alpha ({}^t\vec{z}\,\boldsymbol{\varepsilon}_\mu^{\alpha\prime}\vec{z}) \, \mathrm{d}\alpha. \tag{B.23}$$

Using the definition of $f^\alpha$ and $\boldsymbol{\varepsilon}_\mu^{\alpha\prime}$, we get

$$\mathbf{E}_{\mu_{zz}} = \int_0^{2\pi}\int_0^{\pi} \frac{2\lambda_{100} k^{\mathbf{a}}}{5S} \exp(K\cos\varphi)\left(1 - \frac{3}{2}\sin^2\varphi\right)\sin\varphi \, \mathrm{d}\varphi \, \mathrm{d}\theta \tag{B.24}$$

leading to, after calculation

$$\mathbf{E}_{\mu_{zz}} = \frac{2}{5}\lambda_{100} k^{\mathbf{a}}\left[1 - \frac{3\cosh(K)}{K\sinh(K)} + \frac{3}{K^2}\right]. \tag{B.25}$$

As shown in Appendix D, several estimates can be chosen to calculate the value of $k^{\mathbf{a}}$. For instance, the self-consistent estimate can be used. In the case of iron

$$\tfrac{2}{5}\lambda_{100} k^{\mathbf{a}} = 6.13 \times 10^{-6}. \tag{B.26}$$

## Appendix C. Determination of the magnetic field localization operator

Relations (37) and (38) defining the localization law for the magnetic field are derived from the solution of a magnetostatic problem for an inclusion.

We consider a spherical isotropic magnetic region embedded in an infinite isotropic magnetic medium (Fig. C.1). This medium is submitted to an uniform (at the boundary) magnetic field $\vec{H}^{\infty} = H^{\infty}\vec{x}$.

The behavior law for the spherical region (of radius $R$) is written

$$\vec{M}^{\mathbf{I}} = \chi^{I}\vec{H}^{\mathbf{I}}. \tag{C.1}$$

The behavior law for the infinite medium is written

$$\vec{M}^{\mathrm{o}} = \chi^{\mathrm{o}}\vec{H}^{\mathrm{o}}. \tag{C.2}$$

Without any current density, the Maxwell equations can be written

$$\begin{cases} \operatorname{div}\vec{B} = 0, & \text{where } \vec{B} \text{ denotes the magnetic induction,} \\ \vec{\operatorname{rot}}\,\vec{H} = \vec{0}, & \text{where } \vec{H} \text{ denotes the magnetic field.} \end{cases} \tag{C.3}$$

Under these conditions, the magnetic field can be derived from a scalar potential:

$$\vec{H} = -\vec{\operatorname{grad}}\,\varphi. \tag{C.4}$$

Applying the isotropic behavior law ($\vec{B} = \mu\vec{H}$) leads to the Poisson equation for the potential:

$$\Delta\varphi = 0. \tag{C.5}$$

The solutions for the potential $\varphi$ can be written

$$\begin{cases} \varphi^{\mathrm{I}} = -H^{\mathrm{I}}\, r\cos\theta, & \text{inside the sphere,} \\ \varphi^{\mathrm{o}} = -H^{\infty} r\left(1 - \dfrac{k}{r^3}\right)\cos\theta, & \text{outside the sphere,} \end{cases} \tag{C.6}$$

$H^{\infty}$ being the value for the magnetic field very far from the inclusion. The magnetic field can then be written, following Eq. (C.4):

- Inside the sphere:

$$\vec{H}^{\mathbf{I}} = H^{\mathrm{I}}\vec{x}. \tag{C.7}$$

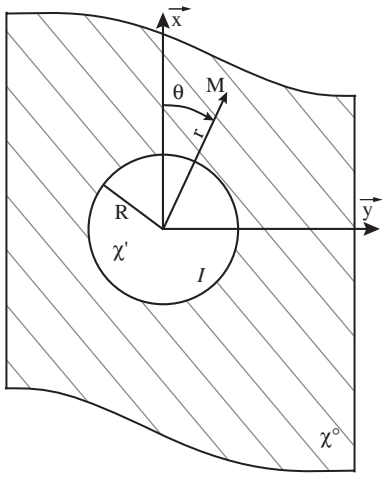


Fig. C.1. Schematic representation of the inclusion problem.

- Outside the sphere:

$$\vec{H}^{\mathrm{o}} = H^{\infty}\left[\left(1+\frac{k}{r^3}(3\cos^2\theta-1)\right)\vec{x}+\frac{3k}{r^3}\cos\theta\sin\theta\,\vec{y}\right]. \tag{C.8}$$

The boundary conditions at the interface of the inclusion give ($\vec{n}$ is the unit vector normal to the sphere surface):

(a) For $\theta=\pi/2$ and $r=R$:

$$[\vec{H}]\wedge\vec{n}=0 \;\Rightarrow\; H^{\mathrm{I}} = H^{\infty}\left(1-\frac{k}{R^3}\right), \tag{C.9}$$

where the symbol $[\vec{H}]$ denotes the jump of $\vec{H}$ through the surface ($[\vec{H}]=\vec{H}^{\mathrm{ext}}-\vec{H}^{\mathrm{int}}$).

From Eq. (C.9) we can deduce

$$k=\left(1-\frac{H^{\mathrm{I}}}{H^{\infty}}\right)R^3. \tag{C.10}$$

(b) For $\theta=0$ and $r=R$

$$\begin{aligned}[\vec{B}].\vec{n}=[\vec{H}+\vec{M}].\vec{x}=0 \;&\Rightarrow\; M^{\mathrm{I}}+H^{\mathrm{I}}=M^{\mathrm{o}}(0,R)+H^{\mathrm{o}}(0,R)\\ &\Rightarrow\; M^{\mathrm{I}}+H^{\mathrm{I}}=(\chi^{\mathrm{o}}+1)H^{\infty}\left(1+\frac{2k}{R^3}\right).\end{aligned} \tag{C.11}$$

Replacing the value of $k$ in Eq. (C.11) leads to

$$M^{\mathrm{I}}+H^{\mathrm{I}}=(\chi^{\mathrm{o}}+1)H^{\infty}\left(3-\frac{2H^{\mathrm{I}}}{H^{\infty}}\right) \tag{C.12}$$

that can also be written:

$$M^{\mathrm{I}}+3H^{\mathrm{I}}+2\chi^{\mathrm{o}}H^{\mathrm{I}}=2\chi^{\mathrm{o}}H^{\infty}+M^{\infty}+3H^{\infty} \tag{C.13}$$

finally leading to the expression

$$H^{\mathrm{I}}-H^{\infty}=\frac{1}{3+2\chi^{\mathrm{o}}}(M^{\infty}-M^{\mathrm{I}}). \tag{C.14}$$

As both magnetization and magnetic fields appearing in Eq. (C.14) are parallel to the direction $\vec{x}$, this relation can be written in a vectorial way

$$\vec{H}^{\mathbf{I}}-\vec{H}^{\infty}=\frac{1}{3+2\chi^{\mathrm{o}}}(\vec{M}^{\infty}-\vec{M}^{\mathbf{I}}). \tag{C.15}$$

This relation justifies the choice made for relation (37), and the particular value of $N_{\mathrm{c}}$ in Eq. (38).

## Appendix D. Magnetic saturation for isotropic polycrystal

The case of infinite isotropic polycrystal is interesting because it allows to obtain analytical results to the homogenization problem when magnetic saturation is reached. Such a configuration can help to define the parameters sensibility of the model.

The considered material is an isotropic polycrystal. Each grain exhibits a cubic crystalline symmetry. All crystallographic orientations are equiprobable, randomly distributed in the material, and the grains are equiaxial, so that the macroscopic behavior is isotropic.

### *D.1. Elastic behavior*

The determination of the effective stiffness tensor of an isotropic polycrystal is a classical problem (see for example Bornert et al., 2007) rapidly summarized hereafter. Isotropic stiffness tensor is defined by two

constants: the shear modulus $\mu$ and the compressibility modulus $k$ are often chosen. The stiffness tensor is then written

$$\mathbb{C} = 2\mu\mathbb{K} + 3k\mathbb{J}. \tag{D.1}$$

The stiffness tensor of a cubic single crystal is written using three constants

$$\mathbb{C}^I = 2\mu_a^I\mathbb{K}^a + 2\mu_b^I\mathbb{K}^b + 3k^I\mathbb{J}. \tag{D.2}$$

The base tensors are defined as

$$\begin{aligned} &J_{ijkl} = \frac{1}{3}\delta_{ij}\delta_{kl}, \quad P_{ijkl} = \delta_{ij}\delta_{kl}\delta_{ik}, \\ &\mathbb{K}^a = \mathbb{P} - \mathbb{J}, \quad \mathbb{K}^b = \mathbb{I} - \mathbb{P}, \\ &\mathbb{K} = \mathbb{K}^a + \mathbb{K}^b = \mathbb{I} - \mathbb{J}. \end{aligned} \tag{D.3}$$

Several hypotheses can be made to determinate the polycrystal effective elastic properties.

Voigt and Reuss hypotheses (respectively, uniform strain and uniform stress within the material) leads to

$$\begin{cases} \mu^{\mathbf{V}} = \dfrac{2\mu_a^I + 3\mu_b^I}{5}, \\ \mu^{\mathbf{R}} = \dfrac{5\mu_a^I\mu_b^I}{3\mu_a^I + 2\mu_b^I}. \end{cases} \tag{D.4}$$

We can also calculate the Hashin and Shtrikman bounds

$$\begin{cases} \mu^{\mathbf{HS}+} = \dfrac{\mu_b^I(3k^I(16\mu_a^I + 9\mu_b^I) + 4\mu_b^I(19\mu_a^I + 6\mu_b^I))}{\mu_b^I(57k^I + 64\mu_b^I) + 18\mu_a^I(k^I + 2\mu_b^I)}, \\ \mu^{\mathbf{HS}-} = \dfrac{\mu_a^I(3k^I(6\mu_a^I + 19\mu_b^I) + 4\mu_a^I(4\mu_a^I + 21\mu_b^I))}{\mu_a^I(63k^I + 76\mu_a^I) + 12\mu_b^I(k^I + 2\mu_a^I)}. \end{cases} \tag{D.5}$$

The self-consistent estimates can also be obtained, verifying the following third-order polynomial equation:

$$8\mu^{\mathbf{SC}^3} + (9k^I + 4\mu_a^I)\mu^{\mathbf{SC}^2} - (12\mu_a^I\mu_b^I + 3k^I\mu_b^I)\mu^{\mathbf{SC}} - 6k^I\mu_a^I\mu_b^I = 0. \tag{D.6}$$

In the case of iron

$$\mu_a^I = 48\,\mathrm{GPa}, \quad \mu_b^I = 116\,\mathrm{GPa}, \quad \text{and} \quad k^I = 174\,\mathrm{GPa} \tag{D.7}$$

leading to the results presented in Table D.1.

All these estimates leads to the same compressibility modulus for the polycrystal

$$k^{\mathbf{V}} = k^{\mathbf{R}} = k^{\mathbf{HS}+} = k^{\mathbf{HS}-} = k^{\mathbf{SC}} = k^I. \tag{D.8}$$

Fig. D.1 shows the sensibility of the result to the single crystal anisotropy.

As expected, the more anisotropic the single crystal is, the more different the estimate becomes. They are of course equal when the single crystal is isotropic. In the case of iron, all these estimates are still quite similar.

### *D.2. Saturation magnetostriction strain*

The magnetic saturation state enables to calculate an analytical form for the macroscopic strain. The material being magnetized at saturation, the magnetization in the material is uniformly aligned along the external field direction, and its norm is $M_s$. Under these conditions the magnetostriction strain in each grain is

Table D.1
Several estimates for the shear modulus of an isotropic iron polycrystal

| | Reuss | HS− | Self-consistent | HS+ | Voigt |
|---|---|---|---|---|---|
| $\mu^{\mathbf{eff}}$ | 74.0 GPa | 80.4 GPa | 82.1 GPa | 83.1 GPa | 88.8 GPa |

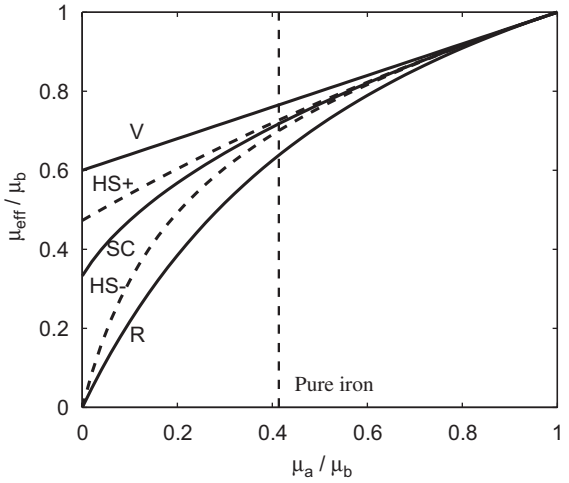


Fig. D.1. Several estimates for the shear modulus of an isotropic polycrystal depending on the single crystal anisotropy—Voigt (V), Reuss (R), Hashin and Shtrikman (HS+ and HS−) and self-consistent (SC) estimates.

uniform and is written, in the crystallographic frame

$$\boldsymbol{\varepsilon}_{\mu}^{I}=\frac{3}{2}\begin{pmatrix}\lambda_{100}(\gamma_1^2-\frac{1}{3}) & \lambda_{111}\gamma_1\gamma_2 & \lambda_{111}\gamma_1\gamma_3\\ \lambda_{111}\gamma_1\gamma_2 & \lambda_{100}(\gamma_2^2-\frac{1}{3}) & \lambda_{111}\gamma_2\gamma_3\\ \lambda_{111}\gamma_1\gamma_3 & \lambda_{111}\gamma_2\gamma_3 & \lambda_{100}(\gamma_3^2-\frac{1}{3})\end{pmatrix}_{\mathrm{CF}}. \tag{D.9}$$

From a macroscopic point of view, the magnetostriction strain can be obtained by the resolution of a thermo-elasticity problem

$$\boldsymbol{E}_{\mu_{\mathbf{sat}}}=\langle {}^{t}\mathbb{B}^{I}\colon\boldsymbol{\varepsilon}_{\mu}^{I}\rangle, \tag{D.10}$$

$\mathbb{B}^{I}$ is the stress concentration tensor and $\langle\cdot\rangle$ denotes the averaging operation over the volume.

The magnetostriction strain being isochore (Du Trémolet de Lacheisserie, 1993), and the macroscopic behavior being isotropic, the magnetostriction strain tensor is written

$$\boldsymbol{E}_{\mu}=\boldsymbol{E}_{\mu}^{\parallel}\begin{pmatrix}1 & 0 & 0\\ 0 & -\frac{1}{2} & 0\\ 0 & 0 & -\frac{1}{2}\end{pmatrix},\quad \boldsymbol{E}_{\mu}^{\parallel}\text{ being a function of the magnetic field.} \tag{D.11}$$

The analytical calculation of $\boldsymbol{E}_{\mu_{\mathbf{sat}}}$ finally leads to the following form for $\boldsymbol{E}_{\mu_{\mathbf{sat}}}^{\parallel}$ (the component of $\boldsymbol{E}_{\mu_{\mathbf{sat}}}$ parallel to the applied magnetic field):

$$\boldsymbol{E}_{\mu_{\mathbf{sat}}}^{\parallel}=\tfrac{2}{5}\lambda_{100}k^{\mathbf{a}}+\tfrac{3}{5}\lambda_{111}k^{\mathbf{b}}. \tag{D.12}$$

As for the shear modulus, different estimates can be obtained, leading to different values for $k^{\mathbf{a}}$ and $k^{\mathbf{b}}$.

Table D.2
Several estimates for the saturation magnetostriction strain of an isotropic iron polycrystal

| | Reuss | HS− | Self-consistent | HS+ | Voigt |
|---|---|---|---|---|---|
| $\boldsymbol{E}^{\parallel \mathbf{sat}}_{\mu_{\mathbf{sat}}}$ | $-4.20\times10^{-6}$ | $-7.90\times10^{-6}$ | $-8.75\times10^{-6}$ | $-9.25\times10^{-6}$ | $-11.9\times10^{-6}$ |

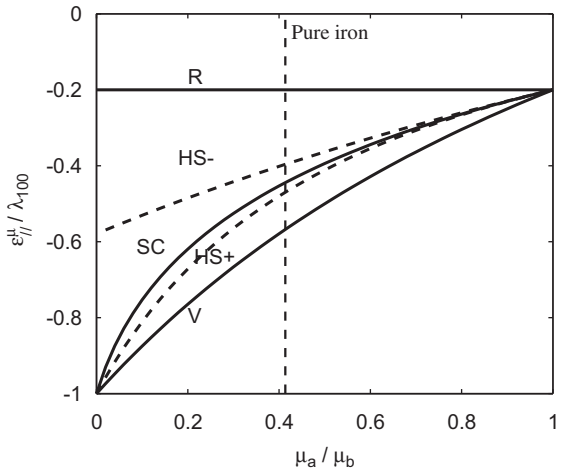


Fig. D.2. Several estimates for the saturation magnetostriction strain depending on the single crystal elastic anisotropy—Voigt (V), Reuss (R), Hashin and Shtrikman (HS+ and HS−) and self-consistent (SC) estimates.

The Voigt and Reuss hypotheses leads to

$$\boldsymbol{E}^{\parallel \mathbf{V}}_{\mu_{\mathbf{sat}}} = \frac{2\mu_a^I\lambda_{100} + 3\mu_b^I\lambda_{111}}{2\mu_a^I + 3\mu_b^I} \quad \text{and} \quad \boldsymbol{E}^{\parallel \mathbf{R}}_{\mu_{\mathbf{sat}}} = \frac{2\lambda_{100} + 3\lambda_{111}}{5}. \tag{D.13}$$

Hashin and Shtrikman and self-consistent estimates can also be obtained (leading to more complicated expressions for $k^{\mathbf{a}}$ and $k^{\mathbf{b}}$).

In the case of iron, we have

$$\lambda_{100} = 21\times10^{-6} \quad \text{and} \quad \lambda_{111} = -21\times10^{-6}. \tag{D.14}$$

The corresponding estimates for the saturation magnetostriction strain are given in Table D.2.

Fig. D.2 shows the sensibility of this result to the single crystal elastic anisotropy.

As expected, all these estimates give the same result when the single crystal is isotropic.

Fig. D.3 shows the saturation magnetostriction strain depending on the magnetostrictive anisotropy of the single crystal. When the single crystal is isotropic, all these estimates are equal. But they rapidly become different when the anisotropy increases. For specific cases, different estimates can lead to different signs for the strain. A situation of elastic isotropy or magnetostrictive anisotropy lead to great simplifications, and give identical estimates whatever the chosen hypotheses (lower and upper bounds are equal). The divergence of these estimates appear as a result of the combination of both elastic and magnetostrictive anisotropy.

### *D.3. Maximum magnetostriction strain*

Maximum magnetostriction strain is obtained, for a material with high level of magnetocrystalline anisotropy, when the wall displacements are stabilized and the magnetization rotation mechanism not started (we suppose here $\lambda_{100} > \lambda_{111}$). Assuming that these two mechanisms are successive (and not simultaneous as they are actually), the maximal magnetostriction strain is obtained by prohibiting in the modeling of the

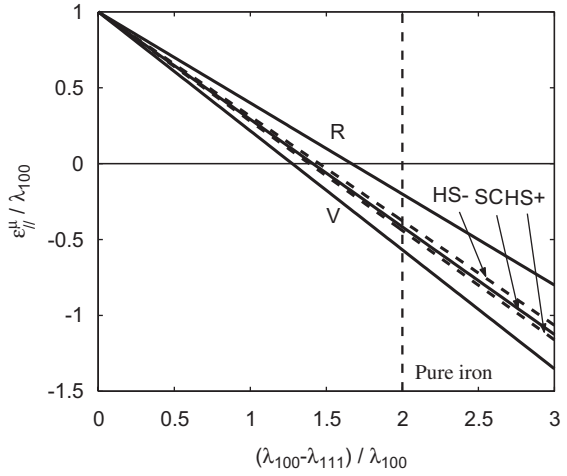


Fig. D.3. Several estimates for the saturation magnetostriction strain depending on the single crystal magnetostrictive anisotropy—Voigt (V), Reuss (R), Hashin and Shtrikman (HS+ and HS−) and self-consistent (SC) estimates.

Table D.3
Several estimates for the maximum magnetostriction strain of an isotropic iron polycrystal

| | Reuss | HS− | Self-consistent | HS+ | Voigt |
|---|---|---|---|---|---|
| $\boldsymbol{E}^{\parallel}_{\mu_{\mathbf{max}}}$ | $8.40 \times 10^{-6}$ | $6.55 \times 10^{-6}$ | $6.13 \times 10^{-6}$ | $5.87 \times 10^{-6}$ | $4.54 \times 10^{-6}$ |

rotation mechanism, i.e. by giving arbitrary high values for the anisotropy constants. For the calculation of analytical values presented in the previous section, it is equivalent to use $\lambda_{111} = 0$ in Eq. (D.12).

Assuming that the relations obtained in the case of magnetic saturation are still valid (even if the magnetization is no more uniform within the material), we obtain several estimates for the maximum magnetostriction strain

$$\boldsymbol{E}_{\mu_{\mathbf{max}}} = \frac{2}{5}\lambda_{100} k^{\mathbf{a}} \begin{pmatrix} 1 & 0 & 0 \\ 0 & -\frac{1}{2} & 0 \\ 0 & 0 & -\frac{1}{2} \end{pmatrix}. \tag{D.15}$$

Results are listed in Table D.3.

## References

Appino, C., Durin, G., Basso, V., Beatrice, C., Pasquale, M., Bertotti, G., 1999. Effect of stress anisotropy on hysteresis and Barkhausen noise in amorphous materials. J. Appl. Phys. 85 (8), 4412–4414.

Azoum, K., Besbes, M., Bouillault, F., 2004. Three dimensional finite element model of magnetostriction phenomena using coupled constitutive laws. Int. J. Appl. Electromagn. Mech. 19, 367–371.

Bernard, Y., Ossart, F., 2004. Comparison between two models of magnetic hysteresis accounting for stress. Int. J. Appl. Electromagn. Mech. 19, 551–556.

Berveiller, M., Zaoui, A., 1978. An extension of the self-consistent scheme to plastically-flowing polycrystals. J. Mech. Phys. Solids 26 (5–6), 325–344.

Bornert, M., Bretheau, T., Gilormini, P., 2007. Homogenization in Mechanics of Material. Iste Publishing Company.

Bozorth, R.M., 1951. Ferromagnetism. Van Nostrand, Princeton, NJ.

Bruggeman, D.A.G., 1935. Berechnung verschiedener physikalischer konstanten von heterogenen substanzen. Annalen der Physik 5 (24), 636–664.

Buiron, N., 2000. Modélisation multi-échelle du comportement magnéto-mécanique couplé des matériaux ferromagnétiques doux. PhD Thesis, Ecole Normale Supérieure de Cachan, France.
Buiron, N., Hirsinger, L., Billardon, R., 1999. A multiscale model for magneto-elastic couplings. J. Phys. IV 9, 139–141.
Chikazumi, S., 1997. Physics of Ferromagnetism, second ed. Clarendon Press, Oxford.
Cullity, B.D., 1972. Introduction to Magnetic Materials. Addison-Wesley Publishing Company, London.
Daniel, L., Hubert, O., Ossart, F., Billardon, R., 2003. Experimental analysis and multiscale modelling of the anisotropic mechanical and magnetostrictive behaviours of electrical steels. J. Phys. IV 105, 247–253.
Daniel, L., Hubert, O., Billardon, R., 2004. Multiscale modelling of the magnetostrictive behaviour of electrical steels—demagnetising surface effect and texture gradient. Int. J. Appl. Electromagn. Mech. 19, 293–297.
Daniel, L., Hubert, O., Vieille, B., 2007. Multiscale strategy for the determination of magneto-elastic behaviour: discussion and application to Ni–Zn ferrites. Int. J. Appl. Electromagn. Mech. 25, 31–36.
DeSimone, A., 1993. Energy minimizers for large ferromagnetic bodies. Arch. Ration. Mech. Anal. 125, 99–143.
DeSimone, A., James, R.D., 2002. A constrained theory of magnetoelasticity. J. Mech. Phys. Solids 50, 283–320.
DeSimone, A., Kohn, R.V., Müller, S., Otto, F., 2000. Magnetic microstructures—a paradigm of multiscale problems. In: Ball, J.M., Hunt, J.C.R. (Eds.), ICIAM 99. Oxford University Press, Oxford, pp. 175–190.
Du Trémolet de Lacheisserie, E., 1993. Magnetostriction—Theory and Applications of Magnetoelasticity. CRC Press, Boca Raton.
Eshelby, J.D., 1957. The determination of the elastic field of an ellipsoidal inclusion, and related problems. Proc. R. Soc. London A 421, 376.
Gilormini, P., 1995. Insuffisance de l'extension classique du modèle autocohérent au comportement non linéaire. C. R. Acad. Sci. Paris, Série IIb 320, 115–122.
Haug, A., Huber, J.E., Onck, P.R., Van der Giessen, E., 2007. Multi-grain analysis versus self-consistent estimates of ferroelectric polycrystals. J. Mech. Phys. Solids 55 (3), 648–665.
He, S., 1999. Modélisation et simulation numérique de matériaux magnétostrictifs. PhD Thesis, Université Pierre et Marie Curie, France.
Hill, R., 1965. Continuum micro-mechanics of elastoplastic polycrystals. J. Mech. Phys. Solids 13, 89–101.
Hirsinger, L., Barbier, G., Gourdin, C., Billardon, R., 2000. Application of the internal variable formalism to the modelling of magneto-elasticity. In: Yang, J.S., Maugin, G.A. (Eds.), Mechanics of Electromagnetic Materials and Structures. IOS Press, pp. 54–67.
Huber, J.E., Fleck, N.A., Landis, C.M., McMeeking, R.M., 1999. A constitutive model for ferroelectric polycrystals. J. Mech. Phys. Solids 47 (8), 1663–1697.
Hubert, A., Schäfer, R., 1998. Magnetic Domains. Springer, Berlin.
Hubert, O., Daniel, L., Billardon, R., 2003. Multiscale modelling and demagnetising surface effect: application to the prediction of magnetostriction of Grain Oriented silicon irons. In: Proceedings of the 16th Soft Magnetic Materials Conference.
James, R., Kinderlehrer, D., 1990. Frustration in ferromagnetic materials. Cont. Mech. Therm. 2, 215–239.
Jiles, D.C., 1991. Introduction to Magnetism and Magnetic Materials. Chapman & Hall, London.
Joule, J.P., 1847. On the effects of magnetism upon the dimensions of iron and steel bars. Philos. Mag. Sér. 3 30 (199), 76–87.
Kuruzar, M.E., Cullity, B.D., 1971. The magnetostriction of iron under tensile and compressive tests. Int. J. Magn. 1, 323–325.
Lagoudas, D.C., Entchev, P.B., Popov, P., Patoor, E., Brinson, L.C., Gao, X., 2006. Shape memory alloys, part II: modeling of polycrystals. Mech. Mater. 38 (5–6), 430–462.
McClintock, F.A., Argon, A.S., 1966. Mechanical Behavior of Materials. Addison-Wesley, New York.
Mura, T., 1982. Micromechanics of Defects in Solids. Martinus Nijhoff Publishers, Dordrecht, MA.
Patoor, E., Lagoudas, D.C., Entchev, P.B., Brinson, L.C., Gao, X., 2006. Shape memory alloys, part I: general properties and modeling of single crystals. Mech. Mater. 38 (5–6), 391–429.
Sablik, M.J., Jiles, D.C., 1993. Coupled magnetoelastic theory of magnetic and magnetostrictive hysteresis. IEEE Trans. Magn. 29 (3), 2113–2123.
Vieille, B., Buiron, N., Pellegrini, Y.P., Billardon, R., 2004. Modelling of the magnetoelastic behaviour of a polycrystalline ferrimagnetic material. J. Phys. IV 115, 129.
Webster, W.L., 1925a. The magnetic properties of iron crystals. Proc. R. Soc. London 107A, 496–509.
Webster, W.L., 1925b. Magnetostriction in iron crystals. Proc. R. Soc. London 109A, 570–584.